

A Computational Study of the Diels–Alder Reaction of Ethyl-*S*-lactyl Acrylate and Cyclopentadiene. Origins of Stereoselectivity

Snezhana M. Bakalova^{†,‡} and A. Gil Santos^{*,†}

REQUIMTE-CQFB, Dep. Química, FCT, Universidade Nova Lisboa, 2829-516 Caparica, Portugal, and
Institute of Organic Chemistry, Bulgarian Academy of Sciences, Acad. G. Bonchev str., block 9,
1113 Sofia, Bulgaria

ags@dq.fct.unl.pt

Received April 27, 2004

The eight diastereoisomeric transition structures of the Diels–Alder addition of ethyl-*S*-lactyl acrylate and cyclopentadiene have been investigated in the gas phase and in solution by HF, MP2, and density functional theory (B3LYP and B3PW91) methods with the 6-31G(d,p) basis set. At all levels of theory used, the *s-cis* transition structures are more stable than the *s-trans* ones. The contribution of the *s-trans* transition structures increases in solution and, although still small, has to be taken in consideration for correct prediction of stereoselectivity. Diastereofacial selectivity is interpreted in terms of electrostatic (weak hydrogen bonding) C=O...H(C) interactions between the carbonyl group(s) of the dienophile and cyclopentadiene in the energetically favored transition structures. *Endo/exo* reaction selectivity is attributed to positive orbital interactions between the diene and the acrylate carbonyl oxygen in the *endo s-cis* transition structures. Ab initio methods reproduce well the experimentally observed trends in both *endo/exo* and diastereofacial selectivity. Density functional calculations in the gas phase correctly reproduce the observed trends in diastereofacial selectivity but single-point MP2 calculations are necessary to reproduce the experimental trend in *endo/exo* selectivity.

Introduction

The Diels–Alder reaction represents one of the most efficient and widely used approaches to carbon–carbon bond formation, and its mechanism has been the subject of a long and, occasionally, fierce debate. Both a concerted mechanism, involving a single, quaziaromatic transition structure, or a stepwise reaction path, involving the formation of an intermediate diradical, have been proposed for the parent reaction between butadiene and ethylene.^{1–4} Nowadays, it is well established that it follows a concerted synchronous mechanism and that the majority of Diels–Alder cycloadditions between asymmetrically substituted dienes and/or dienophiles generally proceed through a concerted, although asynchronous, reaction path.⁵

Hartree–Fock, MP2, CASSCF, CASPT2, density functional, and CBS-QB3 methods have all been applied in modeling of both uncatalyzed and catalyzed Diels–Alder cycloadditions.^{6–8} The detailed theoretical and verifiable mechanistic knowledge (mainly via kinetic isotope effects)

on Diels–Alder reactions has recently evolved into a “standard set of pericyclic reactions for the benchmarking of computational methods for the predictions of activation barriers, reaction energetics and transition state geometries”.⁹

There is a consensus that the medium size 6-31G* basis set is sufficient for reliable optimization of geometries of reactants and transition structures in Diels–Alder reactions and that DFT calculations give more reasonable activation barriers than HF and MP2.^{7–10} However, no clear picture seems to have emerged whether accounting for electron correlation effects during geometry relaxation is mandatory for correct prediction of the stereochemical outcome and, notwithstanding the several decades of computational effort and the many explanations offered, the exact source of stereocontrol for a given cycloaddition is still a source of debate.⁶ Thus, a trend of discarding the attempts to develop a systematic quantum chemical approach and to apply QSAR and mapping

[†] Universidade Nova Lisboa.

[‡] Bulgarian Academy of Sciences.

(1) Li, Y.; Houk, K. N. *J. Am. Chem. Soc.* **1993**, *115*, 7478.

(2) Storer, J. W.; Raimondi, L.; Houk, K. N. *J. Am. Chem. Soc.* **1994**, *116*, 9675.

(3) Houk, K. N.; Gonzalez, J.; Li, Y. *Acc. Chem. Res.* **1995**, *28*, 81.

(4) Goldstein, E.; Beno, B.; Houk, K. N. *J. Am. Chem. Soc.* **1996**, *118*, 6036.

(5) Beno, B. R.; Houk, K. N.; Singleton, D. A. *J. Am. Chem. Soc.* **1996**, *118*, 9984.

(6) Evans, D. A.; Johnson, J. S. In *Comprehensive Asymmetric Catalysis I–III*; Jacobsen, E. N., Pfaltz, A., Yamamoto, H., Eds.; Springer-Verlag: Berlin, Heidelberg, 1999; p 1178.

(7) Wiest, O.; Montiel, D. C.; Houk, K. N. *J. Phys. Chem. A* **1997**, *101*, 8378 and references therein.

(8) Kong, S.; Evanseck, J. D. *J. Am. Chem. Soc.* **2000**, *122*, 10418 and references therein.

(9) Guner, V.; Khuong, K. S.; Leach, A. G.; Lee, P. S.; Bartberger, M. D.; Houk, K. N. *J. Phys. Chem. A* **2003**, *107*, 11445.

(10) Ujaque, G.; Lee, P. S.; Houk, K. N.; Hentemann, M. F.; Danishefsky, S. J. *Chem. Eur. J.* **2002**, *8*, 3423.

techniques^{11,12} to bring the still vague understanding of Diels–Alder stereoselectivity and/or catalysis together into a stereoselection design tool has emerged.

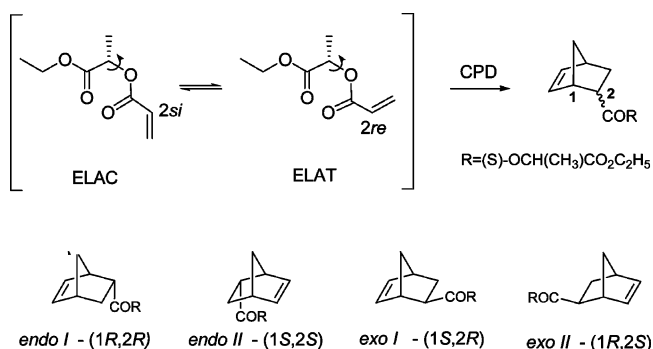
Diels–Alder reactions with acrylates, especially chiral ones, as dienophiles have attracted attention for years.^{13,14} A number of models, based on both experimental and theoretical studies, have been proposed to account for the observed stereoselectivity.¹⁴ In an attempt to contribute to the understanding of the chemical and physical effects behind the stereoselectivity with acrylates, we report here a computational study on the Diels Alder addition of cyclopentadiene, CPD, to ethyl-*S*-lactyl acrylate, ELA, by Hartree–Fock, MP2 and density functional methods. The reaction is found to proceed with moderately high diastereofacial selectivity of up to 85:15.¹⁵ Helmchen et al.¹⁵ have suggested that the observed acrylate enantioface differentiation results from electronic (polar) rather than steric effects, at variance to other chiral acrylates.^{6,13,14,16} Additionally, this cycloaddition is interesting due to the fact that the dienophile has two basic sites (carbonyl groups), which allows both mono- and bidentate complexation with Lewis acid catalysts. Depending on the Lewis acid and the complexation, products of ELA additions can result in different diastereoselectivity.¹⁵ Studies on the mechanism and stereoselectivity of Lewis acid-catalyzed Diels–Alder reactions are now in progress in our group.

Computational Details

Full geometry optimizations have been performed employing HF and MP2 MO theory,¹⁷ as well as density functional theory¹⁸ with two hybrid functionals (Becke's three-parameter exchange functional,¹⁹ combined with one of two correlation functionals, i.e., the hybrids B3LYP²⁰ and B3PW91²¹) with the 6-31G** basis set. The polarization function on hydrogen atoms is added for better description of possible hydrogen bonding involved in the Diels–Alder mechanism to be considered,²² thus enhancing the reliability of envisaged critical energy differences determining stereoselectivity. All calculations have been carried with the GAUSSIAN 98 suite of programs²³ using default optimization criteria. Harmonic vibrational frequencies have been calculated for all located stationary structures to verify whether they are minima or transition structures. Zero-point energies and thermal corrections have been taken from unscaled analytical vibrational frequencies. Reported activation energies include the zero-point correction to energy. Activation free energies are given for 298.15 K.

Geometry optimizations accounting for the solvent are performed using the continuum dielectric solvent model of

SCHEME 1. Stereochemistry of Reactants and Products in the Diels–Alder Cycloaddition of Cyclopentadiene, CPD, to (*S*-Ethyllactyl)acrylate, ELA (*s-cis*, ELAC, and *s-trans*, ELAT)^a



^a The curved arrows point at a C–O single bond to be considered in the conformational analysis.

Tomasi et al. (PCM)^{24–26} as implemented in GAUSSIAN 98. Located stationary structures in solution are verified by calculation of numerical vibrational frequencies.

Results and Discussion

The dienophile reactant, ELA, bears two acrylate face-differentiating groups of distinctly differing electronic type. For the sake of convenience and clarity, we further refer to the face of COOEt as the polar face and to that of CH₃ (H) as the apolar one, respectively.

The *s-cis*/*s-trans* conformational equilibrium in the acryloyl fragment of ELA is important to the analysis of its enantioselective reactions, since the interconversion of the two conformers results in interchange of the *re*- and *si*-faces of the dienophile,¹⁴ as shown for the upper face of the prochiral C₂ atom in Scheme 1. At all levels of theory used, the *s-cis* conformer of (*S*-ethyllactyl)-acrylate, ELAC, is more stable than the *s-trans* one, ELAT, the energy difference being in the range of 0.46–0.78 kcal mol^{–1}. Similar energy preference for the *s-cis* conformation has been previously calculated in the case of methyl acrylate.¹⁴ Further, MO calculations predict that this energy difference is temperature independent, while according to DFT calculations, it decreases at higher temperature.

The asymmetric induction in the studied cycloaddition could be influenced also by rotation about the lactyl–

(11) Lipkowitz, K. B.; D'Hue, C. A.; Sakamoto, T.; Stack, J. N. *J. Am. Chem. Soc.* **2002**, *124*, 14255.

(12) Lipkowitz, K. B.; Pradhan, M. J. *Org. Chem.* **2003**, *68*, 4648.

(13) Ruiz-Lopez, M. F.; Assfeld, X.; Garcia, J. I.; Mayoral, J. A.; Salvatella, L. *J. Am. Chem. Soc.* **1993**, *115*, 8780.

(14) Garcia, J. I.; Mayoral, J. A.; Salvatella, L. *Tetrahedron* **1997**, *53*, 6057.

(15) Poll, T.; Helmchen, G.; Bauer, B. *Tetrahedron Lett.* **1984**, *25*, 2191.

(16) Loncharich, R. J.; Schwartz, T. R.; Houk, K. N. *J. Am. Chem. Soc.* **1987**, *109*, 14.

(17) Hehre, W. J.; Radom, L.; Schleyer, P. v. R.; Pople, J. A. *Ab initio MO Theory*; Wiley: New York, 1986.

(18) Koch, W.; Holthausen, M. C. *A Chemist's Guide to DFT*, 2nd ed.; Wiley: New York, 2001.

(19) Becke, A. D. *J. Chem. Phys.* **1993**, *98*, 5648.

(20) Lee, C.; Yang, W.; Parr, R. G. *Phys. Rev. B* **1988**, *37*, 785.

(21) Perdew, J. P.; Burke, K.; Wang, Y. *Phys. Rev. B* **1996**, *54*, 16533.

(22) Garcia, J. I.; Mayoral, J. A.; Salvatella, L. *Acc. Chem. Res.* **2000**, *33*, 658.

(23) Frisch, M. J.; Trucks, G. W.; Schlegel, H. B.; Scuseria, G. E.; Robb, M. A.; Cheeseman, J. R.; Zakrzewski, V. G.; Montgomery, J. A., Jr.; Stratmann, R. E.; Burant, J. C.; Dapprich, S.; Millam, J. M.; Daniels, A. D.; Kudin, K. N.; Strain, M. C.; Farkas, O.; Tomasi, J.; Barone, V.; Cossi, M.; Cammi, R.; Mennucci, B.; Pomelli, C.; Adamo, C.; Clifford, S.; Ochterski, J.; Petersson, G. A.; Ayala, P. Y.; Cui, Q.; Morokuma, K.; Rega, N.; Salvador, P.; Dannenberg, J. J.; Malick, D. K.; Rabuck, A. D.; Raghavachari, K.; Foresman, J. B.; Cioslowski, J.; Ortiz, J. V.; Baboul, A. G.; Stefanov, B. B.; Liu, G.; Liashenko, A.; Piskorz, P.; Komaromi, I.; Gomperts, R.; Martin, R. L.; Fox, D. J.; Keith, T.; Al-Laham, M. A.; Peng, C. Y.; Nanayakkara, A.; Challacombe, M.; Gill, P. M. W.; Johnson, B.; Chen, W.; Wong, M. W.; Andres, J. L.; Gonzalez, C.; Head-Gordon, M.; Replogle, E. S.; Pople, J. A. *Gaussian 98*, revision A.11.4; Gaussian, Inc.: Pittsburgh, PA, 2002.

(24) Tomasi, J.; Persico, M. *Chem. Rev.* **1994**, *94*, 2027.

(25) Wiberg, K. B.; Keith, T. A.; Frisch, M. J.; Murcko, M. *J. Phys. Chem.* **1995**, *99*, 9072.

(26) Tomasi, J.; Mennucci, B.; Cammi, R.; Cossi, M. In *Computational approaches to biochemical reactivity*; Naray-Szabo, G., Warshel, A., Eds.; Kluwer Academic Publishers: Dordrecht, The Netherlands, 1997; p 1.

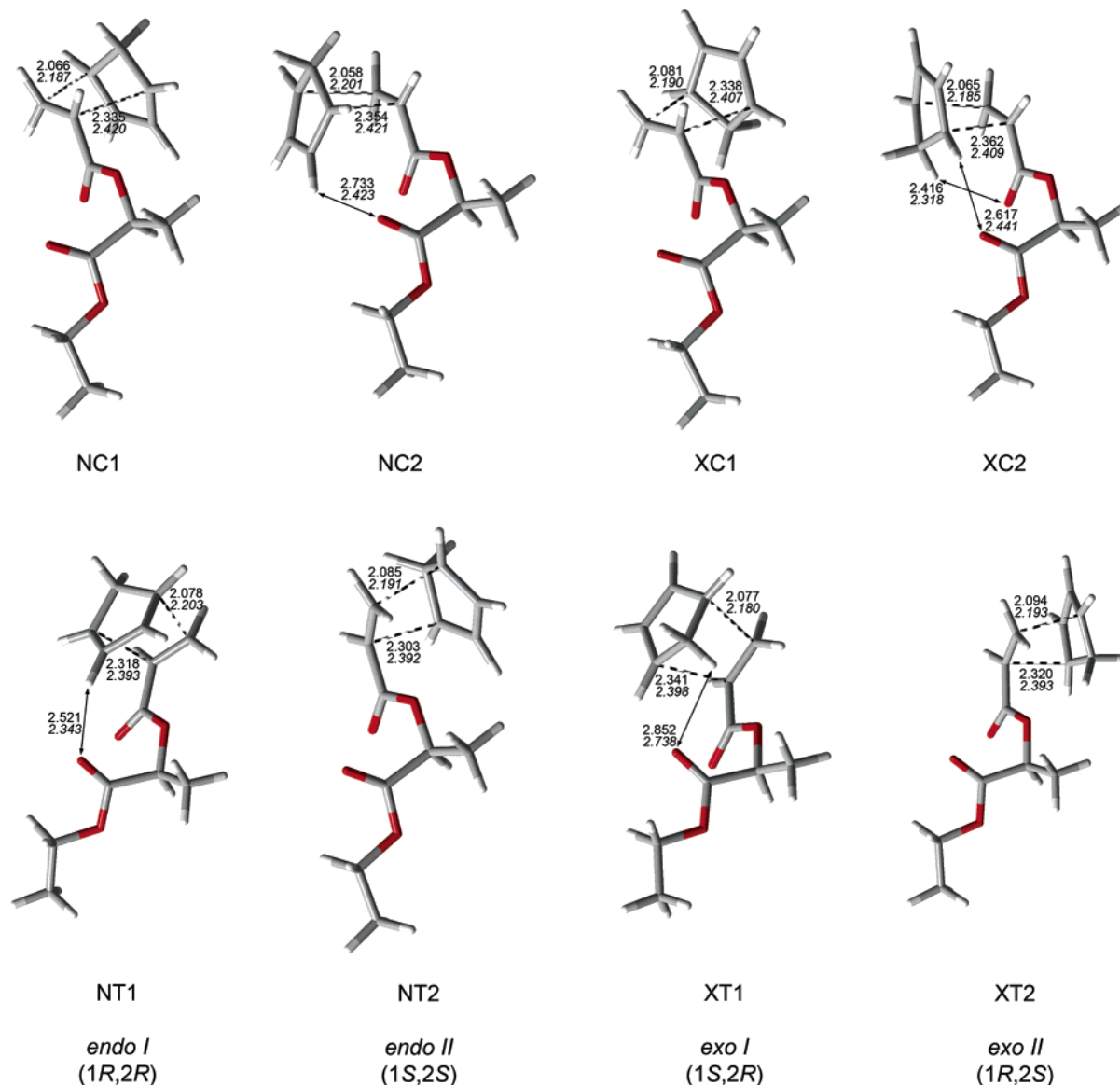


FIGURE 1. Transition structures of the reaction between ELA and CPD in the gas phase, optimized at the HF/6-31G** and MP2/6-31G** level. The lengths of forming C–C bonds are given in angstroms, with the MP2 values in italic.

acrylate C–O–C bonds, as the resulting conformational changes in ELA interchange the acrylate face-differentiating groups. Our conformational search shows that only the rotation about the C–O bond marked in Scheme 1 may be important, as rotation around the adjacent O–C bond leads to a single conformer of ca. 9 kcal mol^{−1} higher energy.

The studied Diels–Alder reaction between ELA and CPD generates two new stereogenic centers and, therefore, produces four diastereoisomeric products (*endo I*, *endo II*, *exo I*, and *exo II*, Scheme 1 and Figure 1). However, if the *s-cis*–*trans* equilibrium in the acrylate fragment is considered as well, the reaction actually has eight possible products, which are rotational isomeric pairs, and eight transition structures (TS), depending on the approach of the diene with respect to the carbonyl group of the dienophile and on the conformation of the latter. In accord with previous conventions,^{8,27,28} the TSs

are denoted as follows: NC1 and NC2 (*endo*, ELAC), XC1 and XC2 (*exo*, ELAC), NT1 and NT2 (*endo*, ELAT), and XT1 and XT2 (*exo*, ELAT).

All located TSs correspond to a concerted, but asynchronous, reaction pathway. The extent of (a)synchronicity is usually measured by means of the difference of the forming bond distances, Δd . We, however, consider the ratio of these distances, d_2/d_1 , a better description of the degree of (a)synchronicity, especially when different methods and/or levels of theory are compared. The comparison of TS geometries calculated at the HF/6-31G** and MP2/6-31G** levels (Figure 1) shows that HF calculations predict both forming C–C bonds systematically shorter than MP2. The MP2 structures are closer to symmetrical, as indicated by Δd and d_2/d_1 values.

DFT calculations—B3LYP as well as B3PW91—give lengths of the shorter forming C–C bonds approximately

(27) Birney, D. M.; Houk, K. N. *J. Am. Chem. Soc.* **1990**, *112*, 4127.

(28) García, J. I.; Martínez-Merino, V.; Mayoral, J. A.; Salvatella, L. *J. Am. Chem. Soc.* **1998**, *120*, 2415.

TABLE 1. Selectivity Ratios, Calculated at the 6-31G** Basis Set Level and Determined from Experiment¹⁵

ratio/method	gas phase								hexane
	HF	MP2//HF	MP2	B3LYP	MP2//B3LYP	B3PW91	MP2//B3PW91	estimated ^a	expt ¹³
<i>endo/exo</i>	59:41	58:42	54:46	28:72	59:41	24:76	57:43	56:44	63:37
<i>endo/endo II</i>	12:88	9:91	11:89	15:85	12:88	25:75	13:87	14:86	20:80
<i>exo/endo II</i>	9:91	9:91	10:90	11:89	14:86	17:83	12:88	11:89	15:85

^a Extrapolated from the experimental data in four solvents.¹⁵

the same as HF calculations, while the longer forming C–C bonds are predicted even longer than by MP2. Thus, DFT predicts the most unsymmetrical TS's among all considered in this paper. For this reason, we have performed an IRC analysis²⁹ at the B3LYP/6-31G** level, which unequivocally shows concertedness of the reaction and justifies the applicability of spin-restricted calculations in this study.

To deduce the theoretical kinetic stereoselectivities, we use the percentage ratios of products, calculated from the activation free energy differences. The results reveal a clear preference for the *s-cis* conformation at all levels of theory used. The percentages of all products indicate a contribution of the *s-trans* TSs to only about 3% of the products. Inspection of geometries shows that the *s-cis* TSs are slightly more asynchronous than the *s-trans* ones; moreover, the length of the more advanced forming bond is shorter in NC and XC, indicating that the *s-cis* TSs appear somewhat later on the reaction coordinate than the *s-trans* ones, NT and XT. According to the Bell–Evans–Polanyi principle, this may help to explain the energetic preference of the reaction for the *s-cis* dienophile over the *s-trans* one. Moreover, reaction through the *s-trans* conformers of ELA would result in opposite to the experimentally observed¹⁵ diastereofacial selectivities (Table 1), as NT1 and XT1 are lower in energy than NT2 and XT2, respectively.

The thermal corrections do not change the relative stabilities of the TSs, with the values of the activation energies relative to NC2, ΔE^\ddagger , being quite close to those of the free activation energies, ΔG^\ddagger . Similar results have been reported previously for the reaction of methylacrylate with cyclopentadiene¹³ and butadiene.¹⁴

The calculations further show that the relative energies of the TSs in each pair of *endo/exo* diastereomers depend on the computational method used. Using the theoretical product percentages, stereoselectivity ratios are calculated and compared to experimental data in Table 1. As both the *endo/exo* and diastereofacial selectivities correlate exceptionally well¹⁵ with the solvent polarity parameter, $E_T(30)^{30}$ ($R^2 > 0.99$), we can also obtain estimates of “gas phase” selectivities (Table 1), extrapolating the experimental results¹⁵ in four solvents. As expected, the values of extrapolated “gas phase” selectivities are close to those in hexane.

Gas-phase MO calculations predict both *endo/exo* and diastereofacial selectivity ratios in very good agreement with experimental observations. The calculated HF product distribution gives the same selectivities as MP2 results, despite the differences in calculated activation parameters and geometries. A similar result has been

reported previously for the concerted cycloaddition between cyclopropene and butadiene, where HF gave the same selectivity predictions as QCISD(T) calculations.³¹ Gas-phase DFT calculations reproduce the observed trends in diastereofacial selectivity correctly but give the opposite prediction for the *endo/exo* selectivity (Table 1), due to an overstabilization of the *exo* relative to the respective *endo* TSs. We further make a simplified qualitative discussion comparing NC2 to XC2, as the results at all levels of theory used show that the contribution of NC2 and XC2 to the products is ca. 90% and the relative energy of these two TSs practically determines the *endo/exo* selectivity. MO calculations predict lower energies of NC2, which agrees with experimentally established preferences.¹⁵ It should be noted that the computed free energy difference between NC2 and XC2 is very small, ca. 0.2 kcal mol^{−1} at HF and MP2//HF, and even smaller for the MP2-optimized structures. About the same energy difference is deduced from experimental data as well. The coincidence in numerical values may be fortuitous, but the identity of their signs shows correct reproducing of experimental trends. DFT results, B3LYP and B3PW91, however, indicate energy differences with the opposite sign, favoring XC2 over NC2. A comparison of the energies of NC2 and XC2, as made above for the MO results, shows that XC2 is favored by 0.6–0.7 kcal mol^{−1} over NC2. Although the NC2–XC2 difference is small, its wrong sign with both used functionals is disappointing. A similar incorrect prediction of DFT for the stereoselectivity of hetero-Diels–Alder reactions between aldehydes and *o*-xylylenes has been reported recently by Houk et al.¹⁰ and attributed to poor account for dispersion interactions within the respective TSs, leading to incorrect geometries and errors of a few kcal mol^{−1} of the otherwise reasonable activation energies.¹⁰

Another failure of B3LYP to predict *endo/exo* selectivities has been reported by Paddon-Row et al. for intramolecular Diels–Alder reaction of hexadienylacrylates.³² The result, appearing among the many reasonable B3LYP predictions of *endo/exo*, as well as diastereofacial Diels–Alder selectivities, has been attributed to the tendency of B3LYP to overestimate the stability of conjugated systems.³² In both cases, MP2 calculations give correct predictions.^{10,32} Paddon-Row et al.³² show further, by single-point MP2 calculations using the B3LYP geometries (MP2//B3LYP), that the reason for the poor B3LYP results lies in the computed B3LYP energies rather than in erroneous geometry optimizations. In this case, the overall error in the B3LYP calculation in comparison to

(29) Gonzalez, C.; Schlegel, H. B. *J. Chem. Phys.* **1989**, *90*, 2154; **1990**, *94*, 5523.

(30) Reichardt, C. *Chem. Rev.* **1994**, *94*, 2319.

(31) Sodupe, M.; Rios, R.; Branchadell, V.; Nicholas, T.; Oliva A.; Dannenberg, J. J. *J. Am. Chem. Soc.* **1997**, *119*, 4232.

(32) Jones, G. A.; Paddon-Row, M. N.; Sherburn, M. S.; Turner, C. I. *Org. Lett.* **2002**, *4*, 3789.

TABLE 2. Selectivity Ratios in Dichloromethane ($\epsilon = 8.9$), Calculated at the 6-31G** Basis Set Level and Determined from Experiment¹⁵

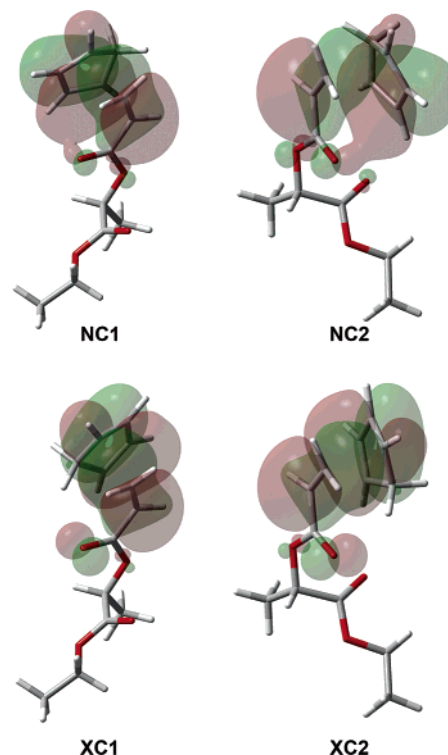
ratio/method	HF	B3LYP	expt
<i>endo</i> / <i>exo</i>	62:38	63:37	76:24
<i>endo II</i> / <i>endo II</i>	46:54	11:89	42:58
<i>exo II</i> / <i>exo II</i>	54:46	28:72	32:68

the MP2/B3LYP one is ca. 1.5 kcal mol⁻¹.³² We use the same approach for the ELA cycloaddition to CPD, which leads to a similar conclusion—MP2/B3LYP and MP2/B3PW91 calculations correctly reproduce the experimentally observed trends in *endo/exo* selectivity (Table 1), despite the large differences in the forming C–C bond lengths, predicted by MP2 and DFT methods. The overall NC2–XC2 free energy difference between the DFT and the respective MP2/DFT values (which are in excellent agreement with the experimentally deduced *endo/exo* energy values) is 0.8–0.9 kcal mol⁻¹ and cannot be neglected.

PCM geometry optimizations in dichloromethane, the most polar solvent used in reported experiments on CPD addition to ELA,¹⁵ show that ELAC remains the major conformer in solution. Both types of theory used, HF and DFT, indicate an extension of the longer forming bond and a shortening of the shorter one, so the asynchronicity of TSs is enhanced in solution relative to the gas phase. The calculated activation energies for the studied DA addition are higher in solution relative to the gas phase. NC2 and XC2 are destabilized by solvation to a greater extent, than their *s-trans* counterparts, while the opposite trend is observed for NC1 and XC1. As a consequence, contrary to the gas phase, NC1 and XC1 are more stable in solution than NC2 and XC2, while NT2 and XT2 are lower in energy than NT1 and XT1. Therefore, consideration of the *s-cis* TSs only would lead to an overestimation of the experimentally observed decrease in stereofacial selectivity with increasing solvent polarity.¹⁵ However, despite the greater contribution of NT2 and XT2 in solution than in the gas phase, the *s-trans* TSs still contribute only about 10% to the products. Thus, in this respect, the theoretically predicted conformational preferences in the cycloaddition of ELA to CPD are different from those in the addition of methyl and (–)-menthyl acrylates to the same diene,^{13,14} in agreement with different observed stereoselectivities. For (–)-menthyl acrylate, the (1*R*,2*R*) cycloadduct is preferentially formed, which requires a preferential approach of the diene from the *si*-face of the dienophile, which is less shielded in its *s-trans* conformation.¹³ For ELA the (1*S*,2*S*) cycloadduct (Scheme 1) is preferentially obtained, in accordance with the computed preferential approach of the diene from the *si*-face of the dienophile in its *s-cis* conformation.

Unlike the gas-phase results, both HF and B3LYP give the same *endo/exo* selectivity prediction in dichloromethane and reproduce the experimentally observed trend of selectivity improvement upon increase of solvent polarity (Table 2).

To understand the role of various interrelated factors on the stereoselectivity of ELA to CPD addition, we consider the following ones for discussion on computational predictions: orbital interactions, electrostatic (hy-

**FIGURE 2.** HOMO-1 orbitals (0.015 e⁻¹ au⁻³) of the *s-cis* TSs: MP2/6-31G**.

drogen bonding) interactions in the TS's between CPD and ELA (one or both of its carbonyl oxygens), relative (a)synchronicity of the TSs, conformational properties of ELA, and solvent polarity dependencies.

Orbital Interactions. The two highest occupied π -orbitals in the TSs are both bonding with respect to the newly forming C–C bonds, HOMO-1 for the shorter and HOMO for the longer, while HOMO-2 is usually a lone pair orbital of the carbonyl oxygen of the lactyl moiety. Minute differences in MO coefficients cannot be inferred as explanations of the *endo* over *exo* selectivity.^{14,22} However, the HOMO-1 of the *endo s-cis* TS's (NC1 and NC2) indicates a stabilizing orbital interaction between the cyclopentadiene carbon atoms 2 and 3 (i.e., the forming double bond of the product) and the acrylate carbonyl oxygen (Figure 2), which is absent in all remaining six transition structures. This can be related to the fact that in NC1 and NC2 the distances between these carbon atoms and the acrylate carbonyl oxygen are in the range of 3.0–3.5 Å, allowing an interaction between them, while in the other TSs the same distances are larger than 4.6 Å.

Electrostatic Interactions. When the dienophile is approached from its polar face, the calculations show attractive electrostatic interactions (nontraditional hydrogen bonds³³) between the carbonyl groups of ELA and the diene (Figure 1, NC2, XC2, NT1, and XT1). In NC2, the interaction is between the lactyl carbonyl oxygen and the hydrogen at the sp² carbon next to the longer forming C–C bond. Although the hydrogen bond is relatively long (2.4 Å at MP2/6-31G**) and deviates from linearity,²⁸ it can account for the observed energy difference of 1.7 kcal

(33) Desiraju, G. R. *Acc. Chem. Res.* **1996**, *29*, 441.

mol⁻¹ between NC1 and NC2. Thus, electron density is supplied inductively from the lone electron pairs of C=O to the π -electronic system to strengthen the incipient C–C bond and lower the HOMO orbital of NC2. A similar stabilizing hydrogen bond interaction is present in NT1 as well. In XC2, there are two such C=O \cdots H(C) contacts. One of these is between the acrylate C=O and the methylene group of CPD (there is a similar interaction in XT1 as well). The other is between the lactyl C=O and the hydrogen at the carbon, participating in the longer incipient C–C bond. Compared to the case of NC1–XC1 pair, with the attack from the nonpolar face of the dienophile, NC2 and XC2 should both be favored due to the mentioned hydrogen bonding interactions, as confirmed by experiment. A similar conclusion can be drawn for the *s-trans* TS's (NT1–XT1 more stable than NT2–XT2) which, given their insignificant relative amounts, practically does not influence the overall reaction stereoselectivity. Polar solvents should weaken the electrostatic interactions, thus destabilizing NC2, XC2, NT1, and XT1 to a greater extent than the other four TS's, which is confirmed by our computational results. Comparison of TS geometries at the HF/6-31G** level shows increase of all these hydrogen bond lengths in dichloromethane relative to gas phase. It should be noted, however, that our calculations do not show a straightforward dependence between the destabilization energy upon solvation and the number of hydrogen bonds present in the corresponding TS.

Conformational Effects. Since we already discussed in detail the *s-cis/s-trans* conformational effects, now we try to apply Cram's rule³⁴ to both ELA conformations, *s-cis* and *s-trans*, and the three possible rotational isomers about the acrylate–lactyl O–C bond (Scheme 1).

In the case of NC1, there is only one more optimizable TS, NC1', which is a higher energy conformer, whereby the *re*-face of ELA becomes the polar one and the lactyl carbonyl oxygen points toward the diene, indeed forming a hydrogen bond, Figure 3. The free energy of NC1' is ca. 2.5 kcal mol⁻¹ higher than that of the lower energy conformer NC1, Figure 1. This result indicates that conformational dependencies in the TS's are more important than internal hydrogen bond stabilization.

The same computational experiment with NC2 also results in a single optimizable TS, NC2', with the medium-sized substituent at the asymmetric center of ELA, CH₃, pointing to the diene. Thus, in this case, the conformational change makes the attacked *si*-face of diene the nonpolar one. In this higher conformer, NC2', all hydrogen bonds disappear, and the additional steric strain brings its relative free energy almost 5 kcal mol⁻¹ higher than that of the parent NC2. With XC1' the additional conformational strain is somewhat compensated by the arising hydrogen bonding of lactyl C=O to a CPD hydrogen, and its destabilization relative to XC1 is only ca. 2 kcal mol⁻¹. Finally, with XC2' we observe no attractive interactions to alleviate the repulsive steric effects in the dienophile part, with the destabilization relative to the lower energy rotamer XC2 increasing to more than 5 kcal mol⁻¹. As observed trends are similar in the *s-trans* series, we will not discuss them in detail.

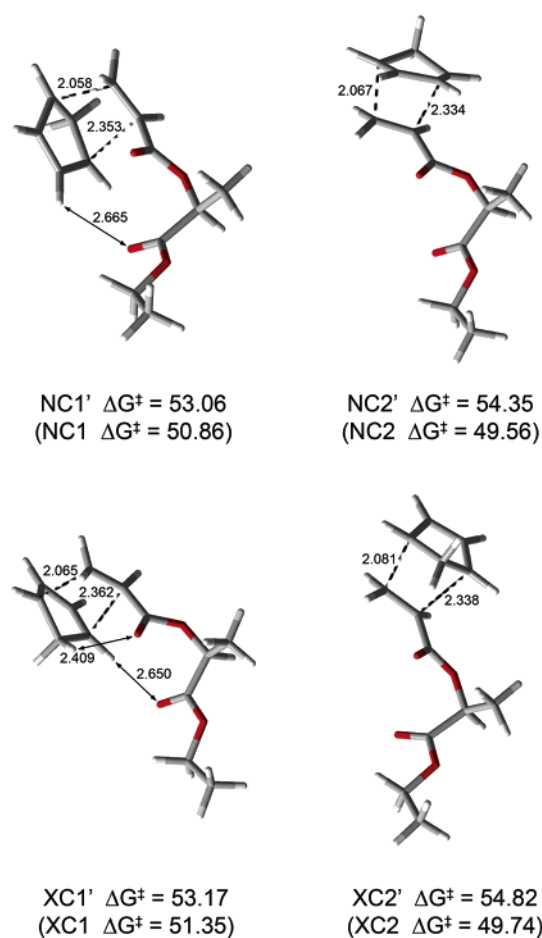


FIGURE 3. Structures, forming bond distances (Å), and activation free energies (kcal mol⁻¹) of the higher energy conformers of the *s-cis* TSs, optimized at the HF/6-31G** level.

Thus, all considered higher energy conformers of the TSs are evidently kinetically insignificant and should not have any measurable contribution to the observed distribution of stereoisomeric products.

Conclusions

Present calculations show that the widely accepted statement that explicit account for electron correlation during the TS optimization leads only to small changes in the respective geometries^{7,27} is not generally applicable. MP2 optimizations lead to the most synchronous TSs, while DFT calculations predict the most unsymmetrical TSs among the considered in this paper. HF and MP2 are found to perform well in predicting Diels Alder *endo/exo* and diastereoface selectivities in the reaction of ELA and, possibly, other dienophiles with faces of different polarity, although HF overestimates and MP2 underestimates activation energies. DFT (B3LYP and B3PW91) calculations give reasonable activation energies, close to the values observed in similar cycloadditions, but do not reproduce well the experimentally observed trends in *endo/exo* selectivity in the gas phase, although the calculated diastereofacial selectivities are reasonable. The results further show that the origin of this discrepancy should not be attributed to the quite

(34) Lowry, T. C.; Richardson, K. S. *Structure and Mechanism in Organic Chemistry*, 3rd ed.; Harper & Row: New York, 1987.

different geometries predicted by DFT methods but, rather, to errors in the computed relative free activation energies. A refinement of energies by SP MP2 calculations using the DFT geometries results in correct predictions of stereoselectivities. Consequently, relative TS energies do not seem sensitive to even rather large geometry changes, when refined at the MP2 level of theory.

The observed stereofacial selectivity, as well as its solvent dependence, can be explained by weak CH \cdots O=C electrostatic interactions in the TSs. A stabilizing orbital overlap between carbon atoms 2 and 3 in the cyclopentadiene moiety and the acrylate carbonyl oxygen in HOMO-1 of the *endo-cis* TSs may account for

the preference for *endo* over *exo* products in Diels–Alder addition of ELA.

Acknowledgment. The financial support of the FCT, Portugal, FEDER (Ref. POCTI/QUI/42983/2001 and Ref. SFRH/BPD/11523/2002) is gratefully acknowledged. We thank Thomas Reuter for installation and maintenance of our Linux cluster.

Supporting Information Available: Tables with HF, MP2, B3LYP, and B3PW91 results for reactants; tables with HF and B3LYP results for products; Cartesian coordinates and total energies of transition structures. This material is available free of charge via the Internet at <http://pubs.acs.org>.

JO049298S